Structure and Bonding of Diiodine Adducts of the Sulfur-Rich Donors 1,3-Dithiacyclohexane-2-thione (ptc) and 4,5-Ethylenedithio-1,3-dithiole-2-thione (ttb)

Francesco Bigoli,[†] Paola Deplano,*[,‡] Andrea Ienco,[§] Carlo Mealli,[§] Maria Laura Mercuri,[‡] Maria Angela Pellinghelli,[†] Gloria Pintus,[‡] Giuseppe Saba,[||] and Emanuele F. Trogu[‡]

Dipartimento di Chimica Generale ed Inorganica, Centro di Studio per la Strutturistica Diffrattometrica del CNR, Università degli Studi di Parma, Viale delle Scienze 78, I-43100 Parma, Italy, Dipartimento di Chimica e Tecnologie Inorganiche e Metallorganiche, Università degli Studi di Cagliari, Cittadella di Monserrato, I09131 Monserrato-Cagliari, Italy, Istituto per lo Studio della Stereochimica ed Energetica dei Composti di Coordinazione (ISSECC, CNR), via Nardi 39, I-50132 Firenze, Italy, and Dipartimento di Scienze Chimiche, Università degli Studi di Cagliari, Cittadella di Monserrato, I09131 Monserrato-Cagliari, Italy

Received February 17, 1999

The reactions of I_2 with ptc and ttb (title ligands) have been investigated in $CHCl_3$ solution at different temperatures by spectrophotometry. A least-squares method procedure provided evidence for the formation of the 1:1 adducts. Crystals of the latter have been analyzed by X-ray diffraction methods (both monoclinic, $P2_1/c$; ptc·I_2, $a = 8.691(6)$ Å, $b = 9.010(6)$ Å, $c = 13.237(5)$ Å, $\beta = 103.43(2)°$, $Z = 4$, $R = 0.0305$; ttb·I_2, $a = 12.090(6)$ Å, $b = 6.433(5)$ Å, $c = 15.731(6)$ Å, $\beta = 99.30(2)°$, $Z = 4$, $R = 0.0419$). Both structures show that the thionic sulfur (in any case a CS_3 group inserted in a ring) is bound almost collinearly with the diiodine molecule. The d(S−I) separations are 2.755(2) and 2.805(3) Å in the ptc·I_2 and ttb·I_2 adducts, respectively, while d(I−I) is practically the same (2.812(2) Å). An evident stereochemical difference is that the S−I−I moiety is nearly coplanar with the CS_3 group in ptc·I_2 while it is upright in ttb·I_2. However, the feature is not expected to cause a major electronic difference. In order to reproduce the structural features, different ab initio approaches have been attempted, with the best results being obtained with the density functional method (DFT). Despite the S−I distances which are slightly longer than the experimental ones (by ca. 0.25 Å), the distribution of filled and empty frontier molecular orbitals (MOs) allows a good interpretation of the visible spectra. Also a rationalization of the σ electronic density distributed over the three centers S−I−I has been attempted by qualitative MO theory (EHMO method). Provided the good agreement with the higher level calculations, the perturbation theory arguments highlight the variable sp hybridization at the central iodine atom as the electronic factor of importance. The strength of the donor (D) affects significantly the redistribution of six electrons over four atomic orbitals, and the classic model is revised as a *four-orbital/six-electron* one. Thus, it is pointed out that a major four-electron repulsion is exerted over the D−I or the I−I linkages with major consequences for their respective lengths.

Introduction

Studies regarding the nature of the interaction between sulfur donors (D) and suitable acceptors such as diiodine in charge-transfer adducts are appealing for both their intrinsic interest and applications. For example, these species are under investigation as powerful reagents for the oxidation of metal powders[1] and also in the field of molecular conductors.[2] On the basis of structural and spectroscopic features of D·I_2 adducts, we have recently proposed[3a,b] to classify them into three main types: D···I−I (**1**);[4] D−I−I (**2**);[3a,5] and D−I^+···I^- (**3**) (the notations ··· and − refer intuitively to intermolecular and intramolecular distances, respectively).[6] In particular, Raman spectroscopy has been shown to have a highly diagnostic value in distinguishing the different types of adducts.

We can summarize the spectral expectations for these compounds as follows: the ν_{I-I} vibration for adducts of type **1** is observed in the region 140−180 cm^{-1} of the Raman spectrum. The frequency is lower than that of I_2 itself (180 cm^{-1} in the solid) in view of the I−I elongation caused by the weak D···I_2 interaction. In the adducts of type **2**, the D−I and I−I distances are comparable and Raman spectra exhibit two peaks ascribable

* Author to whom correspondence should be addressed. Phone: (+39) 070 675 4680. Fax: (+39) 070 675 4499. E-mail: deplano@vaxca1.unica.it.
[†] Università degli Studi di Parma.
[‡] Dipartimento di Chimica e Tecnologie Inorganiche e Metallorganiche, Università degli Studi di Cagliari.
[§] ISSECC, CNR Firenze.
[||] Dipartimento di Scienze Chimiche, Università degli Studi di Cagliari.

(1) Bricklebank, N.; Godfrey, S. M.; McAuliffe, C. A.; Pritchard, R. G. *J. Chem. Soc., Chem. Commun.* **1994**, 695 and references therein. Bigoli, F.; Deplano, P.; Devillanova, F. A.; Lippolis, V.; Mercuri, M. L.; Pellinghelli, M. A.; Trogu; E. F. *Inorg. Chim. Acta* **1998**, *267*, 115. Bigoli, F.; Deplano, P.; Mercuri, M. L.; Pellinghelli, M. A.; Pintus, G.; Serpe, A.; Trogu, E. F. *J. Chem. Soc., Chem. Commun.* **1998**, 2351.
(2) Ferraro, J. R.; Williams, J. M. *Introduction to Synthetic Electrical Conductors*; Academic Press: New York, 1987.
(3) (a) Bigoli, F.; Deplano, P.; Mercuri, M. L.; Pellinghelli, M. A.; Sabatini, A.; Trogu E. F.; Vacca, A. *J. Chem. Soc., Dalton Trans*. **1996**, 3583. (b) Deplano, P.; Ferraro, J. R.; Mercuri, M. L.; Trogu, E. F. *Coord. Chem. Rev.* **1999**, *188*, 71.
(4) Bigoli, F.; Deplano, P.; Mercuri, M. L.; Pellinghelli, M. A.; Sabatini, A.; Trogu, E. F.; Vacca, A. *Can. J. Chem*. **1995**, *73*, 380 and references therein.
(5) Freeman, F.; Ziller, J. W.; Po, H. N.; Keindl, M. C. *J. Am. Chem. Soc*. **1988**, *110*, 2586.
(6) Herbstein, F. H.; Schwotzer, W. *J. Am. Chem. Soc*. **1984**, *106*, 2367.

10.1021/ic9901867 CCC: $18.00
Published on Web 09/23/1999

to the antisymmetrical and symmetrical stretching of the extended D−I−I system. In the adducts of type **3**, where short D−I intramolecular and long I···I distances are found, only one peak ascribable to the D−I vibration is observed in the Raman.

These spectral differences indicate that the simplest MO model where the σ lone pair of the donor (often the HOMO) donates part of its electron density into the relatively low lying σ^* level of I_2 is indeed an oversimplification.[7] Certainly, it fits well to the adducts of type **1** (weaker donors) or to the initial stage of reaction which leads a stronger donor to interact with I_2. Then, as the interatomic D−I and I−I distances vary correlatively so it does the overall MO picture. Accordingly, the system must be described by a model which changes dynamically within limiting forms.

Recently, Hoffmann et al.[8] have illustrated the electronic effects for I_3^- and for the anions of the type X−I−I$^-$ (X = halogen) by applying the concepts of perturbation theory to three-center systems. Essentially the original three-center/four-electron model for the bonding proposed by Pimentel[9] and Rundle[10] is confirmed. Thus one overall σ-bonding and one nonbonding MO (mostly centered at the terminal positions) are populated whereas only the extended antibonding MO is empty. The perturbative effects of the heteroatoms on central or terminal positions have been highlighted. As an extension, the authors suggest that the same type of analysis could be applied to describe the bonding in donor−acceptor adducts of different nature.

The donors investigated in this paper are ptc = 1,3-dithiacyclohexane-2-thione and ttb = 4,5-ethylenedithio-1,3-dithiole-2-thione, depicted in the illustration for clarity. Both

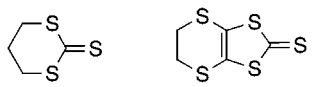

ptc ttb

of these ligands play a variety of coordination modes toward metals[11,12] with a combination of endocyclic and/or terminal and bridging exocyclic sulfur atoms giving rise to polynuclear complexes. ttb is also a precursor of bis(ethylenedithio)-tetrathiofulvalene (BEDT-TTF), a well-known sulfur-rich donor from which superconductors have been obtained.[2] In this type of system, the S···S contacts mostly determine the intermolecular interactions which have been considered to be an essential feature for the conductivity of these sulfur-rich compounds.

The aims of the present study are to check (i) the relative donor capabilities of the sulfur atoms toward diiodine and the type of adducts which are formed; (ii) the response of Raman spectroscopy in diagnosing the nature of the donor−acceptor interaction (importantly, a double-check with the results of the X-ray crystallography can be made); (iii) the capability of ab initio calculations in reproducing the geometries of the adducts; and (iv) the analysis of the frontier MOs (also by using a simpler MO approach such as EHMO) in order to derive a more general model for the variety of interactions between the I_2 and donors of different strength.

Experimental Section

Materials. Reagents and solvents of reagent grade quality were used as furnished by Aldrich. The donors ptc and ttb were prepared according to refs 13 and 14, respectively. Compounds ttb·I_2 and ptc·I_2 were prepared by allowing $CHCl_3$ solutions of the donors and I_2 in a 1:1 molar ratio to stand at room temperature. After several days, lustrous red-brown crystals suitable for X-ray diffraction studies were obtained. The corresponding adducts with IBr have been obtained by a similar procedure using CH_2Cl_2 as solvent and redissolving the obtained solids with hot solvent. By cooling, yellow (ptc·IBr) and orange (ttb·IBr) crystals were isolated.

ptc·I_2. Elemental anal. Found: C, 12.21; H, 1.40; S, 24.27. $C_4H_6S_3I_2$ requires C, 11.89; H, 1.50; S, 23.80. IR (cm^{-1}): 1423vw, 1409vw, 1344w, 1271m, 1232w, 1178w, 1056w, 1015w, 1005w, 988m, 978s, 945vs, 908m, 868vs, 816vw, 657vw, 507w, 480w, 349w, 323w, 295ms, 243w. Raman (cm^{-1}): 2957mw, 2941mw, 2911m, 1273w, 947w, 901w, 867mw, 660w, 644mw, 506m, 479m, 352w, 327w, 285m, 146vs.

ptc·IBr. Elemental anal. Found: C, 13.69; H, 1.60; S, 27.17. $C_4H_6S_3$-IBr requires C, 13.45; H, 1.69; S, 26.93. IR (cm^{-1}): 1422vw, 1409vw, 1383m, 1347w, 1270m, 1228w, 1055vw, 1010w, 984ms, 938ms, 906m, 866s, 820w, 512w, 482w, 349w, 334w, 322w, 300mw, 242w. Raman (cm^{-1}): 2915m, 510m, 482m, 304m, 154vs, 136s, 102m, 84w.

ttb·I_2. Elemental anal. Found: C, 12.89; H, 0.71; S, 34.34. $C_5H_4S_5I_2$ requires C, 12.56; H, 0.84; S, 33.53. IR (cm^{-1}): 1470w, 1410w, 1390w, 1295w, 1260vw, 1180vw, 1130vw, 1070m, 1035vs, 930vw, 910vw, 870w, 680vw, 540w, 460w, 440vw, 360w, 320m. Raman (cm^{-1}): 2959vw, 2921vw, 1462w, 1291vw, 1172vw, 1015 vw, 922vw, 874vw, 637vw, 532w, 457vw, 355vw, 146vs.

ttb·IBr. Elemental anal. Found: C, 14.16; H, 0.81; S, 37.70. $C_5H_4S_5$-IBr requires C, 13.93; H, 0.94; S, 37.18. IR (cm^{-1}): 1423vw, 1409vw, 1344w, 1271m, 1232w, 1178w, 1056w, 1015w, 1005w, 988m, 978s, 945vs, 908m, 868vs, 816vw, 657vw, 507w, 480w, 349w, 323w, 295ms, 243w. Raman (cm^{-1}): 2917m, 1461ms, 538m, 459w, 357w, 327w, 243w, 151vs.

Spectroscopic Measurements. IR Spectra. IR spectra (4000−200 cm^{-1}) were recorded on a Perkin-Elmer model 983 spectrophotometer as KBr pellets; the far-FTIR spectra (400−50 cm^{-1}) have been recorded on a Bruker IFS55 spectrometer working at room pressure and using a flux of dried air.

FT-Raman Spectra. FT-Raman spectra (resolution ±4 cm^{-1}) were recorded on a Bruker RFS100 FTR spectrometer, fitted with an indium−gallium−arsenide detector (room temperature) and operating with an excitation frequency of 1064 nm (Nd:YAG laser). The power level of the laser source was 300 mW for the solution samples and 100 mW for the ligands, and it varied between 20 and 40 mW for the products. The $CHCl_3$ solutions (donors and diiodine in a 1:1 ratio, $c = 3.0 \times 10^{-2}$ mol dm^{-3}) and the solid samples were introduced into a suitable cell (Suprasil 300, HELLMA cell of 0.5 cm thickness) and into a capillary tube, respectively, and then fitted into the compartment designed for a 180° scattering geometry. No sample decomposition was observed during the experiments.

UV−Visible Measurements. Electronic spectra were recorded in $CHCl_3$ solutions with a Cary 5 spectrophotometer equipped with a temperature probe accessory connected to a thermostatable multicell block.

ptc. One set of solutions containing a fixed concentration of the ligand, 5.0×10^{-4} mol dm^{-3}, and variable I_2 concentrations ranging from 5.0×10^{-4} to 2.4×10^{-2} mol dm^{-3} (in the ratios [ptc]:[I_2] = 1:1, 1:2, 1:4, 1:6, 1:8, 1:10, 1:15, 1:20, 1:30, 1:40, 1:50) was prepared, and their spectra were measured at six different temperatures (T = 10−35 °C) in the range 250−460 nm, in 0.1 cm silica cells.

(7) Purcell, K. F.; Kotz, J. C. *Inorganic Chemistry*; Saunders: Philadelphia, 1977.
(8) Landrum, G. A.; Goldberg, N.; Hoffmann, R. *J. Chem. Soc., Dalton Trans.* **1997**, 3605.
(9) Pimentel, G. C. *J. Chem. Phys.* **1951**, *19*, 446.
(10) Hack, R. J.; Rundle, R. E. *J. Am. Chem. Soc.* **1951**, *73*, 4321.
(11) Bellitto, C.; Bigoli, F.; Deplano, P.; Mercuri, M. L.; Pellinghelli, M. A.; Staulo, G.; Trogu, E. F. *Inorg. Chem.* **1994**, *33*, 3005.
(12) Dai, J.; Kuroda-Sowa, T.; Munakata, M.; Maekawa, M.; Suenaga, Y.; Ohno, Y. *J. Chem. Soc., Dalton Trans.* **1997**, 2363. Dai, J.; Kuroda-Sowa, T.; Suenaga, Y.; Wu, L. P.; Yamamoto, M. *Inorg. Chim. Acta* **1997**, *255*, 163.
(13) Sugawara, A.; Sato, T.; Sato, R. *J. Chem. Soc., Dalton Trans.* **1992**, 3145.
(14) Steimecke, G.; Sieler, H. J.; Kirmse, R.; Hoyer, E. *Phosphorus Sulfur Relat. Elem.* **1979**, *7*, 49.

Table 1. Crystallographic Data of Compounds ptc·I_2 and ttb·I_2

	ptc·I_2	ttb·I_2
formula	$C_4H_6I_2S_3$	$C_5H_4I_2S_5$
fw	404.07	478.18
cryst syst	monoclinic	monoclinic
space group	$P2_1/c$ (No. 14)	$P2_1/c$ (No. 14)
a/Å	8.691(6)	12.090(6)
b/Å	9.010(6)	6.433(5)
c/Å	13.237(5)	15.731(6)
β/deg	103.43(2)	99.30(2)
V/Å^3	1008.2(1.0)	1207.4(1.2)
Z	4	4
D_c/(Mg m^{-3})	2.662	2.631
diffractometer	Philips PW 1100	Philips PW 1100
radiation	graphite monochromated	graphite monochromated
wavelength	Mo $K\alpha$ (λ = 0.710 73 Å)	Mo $K\alpha$ (λ = 0.710 73 Å)
F(000)	736	880
temp/K	295	295
cryst size/mm	0.12 × 0.19 × 0.31	0.15 × 0.29 × 0.35
μ/cm^{-1}	67.87	60.23
scan mode	$\theta-2\theta$	$\theta-2\theta$
scan speed/(deg min^{-1})	3−9.6	3−9.6
scan width/deg	1.20 + 0.346 tan θ	1.20 + 0.346 tan θ
θ range for intensity collection/deg	3−27	3−27
data collected	$\pm h,k,l$	$\pm h,k,l$
no. of unique reflns (R_{int})	2192 (0.0308)	2640 (0.0276)
refinement method	full-matrix least-squares on F^2	full-matrix least-squares on F^2
data/restraints/params	2192/0/83	2625/0/109
extinction coeff		0.016(1)
min/max height in final $\Delta\rho$ map	−0.878/0.598 e Å^{-3}	−1.28/1.86 e Å^{-3}
goodness of fit on F^2	0.775	1.227
final R indexes [$I > 2\sigma(I)$]	R1[a] = 0.0305, wR2[b] = 0.0611	R1 = 0.0419, wR2 = 0.1016
R indexes (all data)	R1 = 0.0681, wR2 = 0.0661	R1 = 0.0784, wR2 = 0.1471

[a] $R1 = \sum||F_o| - |F_c||/\sum|F_o|$. [b] $wR2 = [\sum[w(F_o^2 - F_c^2)^2]/\sum[w(F_o^2)^2]]^{1/2}$.

ttb. Two sets of solutions containing respectively (a) a fixed concentration of the ligand (7.5×10^{-4} mol dm^{-3}) and variable I_2 concentrations ranging from 7.5×10^{-4} to 3.75×10^{-2} mol dm^{-3} (in the ratios [ttb]:[I_2] = 1:1, 1:3, 1:5, 1:7, 1:10, 1:15, 1:20, 1:25, 1:30, 1:40, 1:50) in the range 250−360 nm and (b) a fixed concentration of I_2 (5.3×10^{-4} mol dm^{-3}) and variable ttb concentrations ranging from 1.3×10^{-4} to 2.5×10^{-3} mol dm^{-3} (in the ratios [ttb]:[I_2] = 1:0.25, 1:0.5, 1:0.75, 1:1, 1:1.25, 1:1.5, 1:2, 1:3, 1:5) in the range 360−510 nm were prepared, and their spectra were measured at six different temperatures (T = 10−35 °C), in 0.1 cm silica cells.

Calculations. The previously described program SUPERSPEC,[4] derived from SUPERQUAD,[15] has been used to refine the equilibrium constants β and the molar absorptivities ϵ_i simultaneously from the experimental absorbances taken every 10 nanometers at six different temperatures in the range T = 10−35 °C. In the ptc case, data were taken in the 250−460 nm range and the total number of experimental points was 264. In the case of ttb, data were taken in the 250−510 nm range and the total number of experimental points was 217. The values of $\Delta H°$ and $\Delta S°$ were calculated by least-squares fitting of the corresponding ln β versus $1/T$ according to the van't Hoff equation.

X-ray Structural Analyses. Table 1 contains a summary of data collection conditions and results. The check of the standard reflections showed no significant decrease. Intensities were corrected for Lorentz and polarization effects. The empirical absorption correction applied for ptc·I_2 was that following Walker and Stuart[16] (maximum and minimum values: 1.3040 and 0.8041); the correction was that following North et al.[17] for ttb·I_2 by measuring two reflections with a χ value near 90° at different ψ values (0−180° in steps of 10°). The structures were solved via direct methods[18] and then subjected to full-matrix least-squares refinement on F^2 [19] with anisotropic thermal parameters for all of the non-hydrogen atoms excluding the carbon atoms of the ethylene group in the six-membered ring of ttb·I_2. In fact the last two atoms were found to be disordered, and they were inserted in two positions with side occupancy factor of 0.58 and 0.42, respectively, as found from the refinement. Hydrogen atoms were placed in their calculated positions, and their coordinates were fixed in the final refinement as well as their thermal parameters. Scattering factors and corrections for anomalous dispersion effects were those from ref 20. The programs ABSORB,[21] PARST,[22] PLUTO,[23] and ORTEP[24] were used. Calculations were carried out on the ENCORE 91 computer of the Centro di Studio per la Strutturistica Diffrattometrica del CNR (Parma).

Computational Methodology. Three different model chemistries were employed to investigate the molecular structures and the energetics of the ligands and the adducts: the ab initio Hartree−Fock (HF) method, the effective core potential (ECP) approximation, and the density functional method (DFT). The ab initio HF basis set was the highest quality basis set available for iodine in the Gaussian series of quantum mechanical programs[25] as well as in the quantum mechanics module of the molecular modeling software Spartan 4.1.2;[26] this basis is a split valence basis set supplemented by a set of d-type functions on second-

(15) Gans, P.; Sabatini, A.; Vacca, A. *J. Chem. Soc., Dalton Trans*. **1985**, *49*, 1195.
(16) Walker, N.; Stuart, D. *Acta Crystallogr.* **1983**, *39A*, 158.
(17) North, A. C. T.; Phillips, D. C.; Matthews, F. S. *Acta Crystallogr*. **1968**, *24A*, 351.
(18) Sheldrick, G. M. *SHELXS-86: Program for the solution of crystal structures*; Universität Göttingen: Göttingen, Germany, 1986.
(19) Sheldrick, G. M. *SHELX93: Program for crystal structure refinement*; Universität Göttingen: Göttingen, Germany, 1993.
(20) *International Tables for X-ray Crystallography*; Kynoch Press: Birmingham, U.K., 1974; Vol. IV, pp 99−102, 149.
(21) Ugozzoli, F. *Comput. Chem*. **1987**, *11*, 109.
(22) Nardelli, M. *Comput. Chem*. **1983**, *7*, 95.
(23) Motherwell, W. D. S. *PLUTO*; University of Cambridge: Cambridge, U.K., 1976.
(24) Johnson, C. K. ORTEP. Report ORNL-3794, revised; Oak Ridge National Laboratory: Oak Ridge, TN, 1965.
(25) Frisch, M. J.; et al. *Gaussian 94* (revision D.1); Gaussian, Inc.: Pittsburgh, PA, 1995.
(26) *SPARTAN*, version 4.1.2: Wavefunction, Inc., 18401 Von Karman Avenue, Suite 370, Irvine, CA 92612.

row and heavier main group elements.[27] The ECP calculation has been carried out using the LANL2DZ basis set which comprises the Dunning/Huzinaga valence double-ζ D95 basis on first-row atoms[28] and Los Alamos ECP plus double-ζ on Na−Bi.[29] In this method the relativistic effect of the inner electrons of the iodine atoms is partially taken into account. The density functional methods are meeting increasing interest for the description of strongly bonded systems[30,31] and more recently for the study of weak intermolecular interactions.[32,33] The DFT approach is based on the strategy of modeling electron correlation via general functionals of the electron density; here we have used the B3LYP/3-21G** [34−36] method which incorporates contributions from the Hartree−Fock exchange and correlation functional and where the basis set is a split valence Gaussian set with polarization functions on hydrogens, p-type, and d-type (heavy atoms). All calculations have been done by means of the Gaussian 94 suite of programs[25] or the Spartan 4.1.2 molecular modeling package.[26] The latter has been used also to investigate the shape of the molecular orbitals.

In the MO calculations of the extended Hückel type[37] a weighted-modified Wolfsberg−Helmholz formula[38] was used. The package CACAO[39] has the graphic capabilities for the visual analysis of the results and, in the newest version,[39b] includes the possibility of constructing the very useful MOOP (molecular orbital overlap population) diagrams.

Results and Discussion

Crystal and Molecular Structures of the Adducts. Table 1 contains a summary of the conditions for data collection and structure refinement. Final atomic coordinates are reported in Table 2, and bond distances and angles are reported in Table 3.

ptc·I_2. The structure of the molecule of ptc·I_2 and the corresponding atom-labeling scheme are shown in Figure 1. The geometry of the organic molecule is very similar to that previously observed by us as a ligand in Cu(I) and Cu(II) coordination compounds. In the latter, ptc is able to use both the exocyclic and endocyclic sulfur atoms in various arrangements as terminal and bridging donor atoms. Essentially, three different copper derivatives have been characterized: a mixed-valence Cu(I)−Cu(II) trimer, a Cu(I) dimer, and a Cu(I) polymer.[11] Also in the present ptc·I_2 adduct, the SC(S)S moiety maintains planarity together with the carbon atoms bound to the endocyclic sulfur atoms. Thus the six-membered ring, half formed by a three-methylenic chain, assumes the half-boat conformation, only the carbon atom opposite to the C−S(thione) bond being significantly displaced out of CS_3 group least-squares plane (−0.482(9) Å). The electron delocalization within the planar CS_3 group (see bond distances and angles) and the interaction of the exocyclic sulfur atom with one iodine atom of I_2 (S−I separation being 2.755(2) Å) affect the exocyclic C−S distance (1.690(6) Å), which is similar to the endocyclic C−S distances and significantly longer with respect to a double-bond CS distance. The I−I vector, which is quasi collinear with the S−I one [175.42(4)°], is slightly elongated with respect to that in the free I_2 molecule [2.812(1) Å vs 2.715(1) Å].

Table 2. Fractional Atomic Coordinates ($\times 10^4$) with Esd's in Parentheses and Isotropic Thermal Parameters (Å^2 $\times$ 10^3) for the Non-Hydrogen Atoms ptc·I_2 and ttb·I_2

atom	*X*/*a*	*Y*/*b*	*Z*/*c*	*U*
(a) Compound $C_4H_6I_2S_3$ (ptc·I_2)				
I(1)	3374(1)	402(1)	876(1)	35(1)[a]
I(2)	5871(1)	−1204(1)	2138(1)	56(1)[a]
S(1)	1033(2)	1925(2)	−491(1)	47(1)[a]
S(2)	−1686(2)	3703(2)	−660(1)	40(1)[a]
S(3)	−151(2)	2201(2)	1388(1)	50(1)[a]
C(1)	−312(7)	2618(6)	123(4)	30(1)[a]
C(2)	−3119(8)	4232(8)	67(5)	52(2)[a]
C(3)	−2456(11)	4382(10)	1209(6)	80(3)[a]
C(4)	−1838(10)	3047(9)	1739(6)	71(2)[a]
(b) Compound $C_5H_4I_2S_5$ (ttb·I_2)				
I(1)	3092(1)	2690(1)	3305(1)	49(1)[a]
I(2)	4441(1)	6258(1)	3333(1)	72(1)[a]
S(1)	1721(2)	−852(4)	3134(2)	52(1)[a]
S(2)	344(2)	2408(3)	3840(2)	56(1)[a]
S(3)	−530(2)	−1683(4)	3519(2)	56(1)[a]
S(4)	−2657(2)	−951(4)	4188(2)	61(1)[a]
S(5)	−1573(3)	3988(4)	4609(3)	87(1)[a]
C(1)	571(6)	−23(13)	3483(6)	40(2)[a]
C(2)	−1381(6)	24(12)	3981(5)	38(2)[a]
C(3)	−967(7)	1936(13)	4135(6)	47(2)[a]
C(4)	−2986(14)	3388(28)	4229(17)	51(6)
C(5)	−3384(14)	1233(27)	4532(17)	47(5)
C(41)	−2856(20)	3210(37)	4725(22)	50(8)
C(51)	−3446(10)	1465(37)	4173(22)	43(6)

[a] U_{eq} is defined as one-third of the trace of the orthogonalized $\mathbf{U}_{ij}$ tensor.

Table 3. Bond Lengths (Å) and Angles (deg) for ptc·I_2 and ttb·I_2

(a) Compound $C_4H_6I_2S_3$ (ptc·I_2)			
I(1)−I(2)	2.812(1)	S(3)−C(1)	1.690(6)
I(1)−S(1)	2.755(2)	S(3)−C(4)	1.806(7)
S(1)−C(1)	1.690(6)	C(2)−C(3)	1.493(10)
S(2)−C(1)	1.698(6)	C(3)−C(4)	1.433(10)
S(2)−C(2)	1.805(6)		
S(1)−I(1)−I(2)	175.42(4)	S(3)−C(1)−S(2)	128.1(3)
C(1)−S(1)−I(1)	110.8(2)	S(1)−C(1)−S(2)	112.7(3)
C(1)−S(2)−C(2)	107.5(3)	C(3)−C(2)−S(2)	114.3(5)
C(1)−S(3)−C(4)	106.0(3)	C(4)−C(3)−C(2)	115.6(7)
S(3)−C(1)−S(1)	119.2(3)	C(3)−C(4)−S(3)	117.6(6)
(b) Compound $C_5H_4I_2S_5$ (ttb·I_2)			
I(1)−I(2)	2.812(2)	S(5)−C(3)	1.736(9)
I(1)−S(1)	2.805(3)	S(5)−C(4)	1.76(2)
S(1)−C(1)	1.663(8)	S(4)−C(5)	1.79(2)
S(2)−C(1)	1.699(9)	S(5)−C(41)	1.67(2)
S(2)−C(3)	1.748(8)	S(4)−C(51)	1.82(2)
S(3)−C(1)	1.714(8)	C(2)−C(3)	1.34(1)
S(3)−C(2)	1.742(8)	C(4)−C(5)	1.57(3)
S(4)−C(2)	1.744(8)	C(41)−C(51)	1.52(4)
S(1)−I(1)−I(2)	175.43(6)	S(3)−C(2)−C(3)	115.2(6)
C(1)−S(1)−I(1)	102.8(3)	S(4)−C(2)−C(3)	127.9(7)
C(1)−S(2)−C(3)	97.5(4)	S(3)−C(2)−S(4)	116.8(5)
C(1)−S(3)−C(2)	97.8(4)	S(5)−C(3)−C(2)	127.3(6)
C(2)−S(4)−C(51)	99.7(8)	S(2)−C(3)−C(2)	116.2(6)
C(2)−S(4)−C(5)	105.5(6)	S(5)−C(3)−S(2)	116.5(5)
C(3)−S(5)−C(4)	98.1(7)	S(5)−C(4)−C(5)	114.8(16)
C(3)−S(5)−C(41)	106.5(9)	S(4)−C(5)−C(4)	114.4(15)
S(1)−C(1)−S(2)	126.3(5)	S(5)−C(41)−C(51)	121(2)
S(1)−C(1)−S(3)	120.4(5)	S(4)−C(51)−C(41)	115(2)
S(2)−C(1)−S(3)	113.2(5)		

(27) Binkley, J. S.; Pople, J. A.; Hehre, W. J. *J. Am. Chem. Soc.* **1980**, *102*, 939 and references therein.
(28) Dunning, T. H., Jr.; Hay, P. J. *Modern Theoretical Chemistry*; Schaefer, H. F., III, Ed.; Plenum: New York, 1976; p 1.
(29) Hay, P. J.; Wadt, W. R. *J. Chem. Phys.* **1985**, *82*, 270 and references therein.
(30) Salahub, D. R.; Fournier, R.; Mlynarski, P.; Papai, I.; St. Amant, A. In *Density Functional Methods in Chemistry*; Labanowski, J., Andzelm, J., Eds.; Springer: New York, 1991.
(31) Ziegler, T. *Chem. Rev.* **1991**, *91*, 651.
(32) Kieninger, M.; Suhay, S. *Int. J. Quantum Chem.* **1994**, *52*, 465.
(33) Ruiz, E.; Salahub, D. R.; Vela, A. *J. Am. Chem. Soc.* **1995**, *117*, 1141.
(34) Becke, A. D. *J. Chem. Phys.* **1993**, *98*, 5648.
(35) Lee, C.; Yang, W.; Parr, R. G. *Phys. Rev.* **1988**, *B37*, 785.
(36) Miehlic, B.; Savin, A.; Stoll, H.; Preuss, H. *Chem. Phys. Lett.* **1989**, *157*, 200.
(37) (a) Hoffmann, R.; Lipscomb, W. N. *J. Chem. Phys.* **1962**, *36*, 2872. (b) Hoffmann, R.; Lipscomb, W. N. *J. Chem. Phys.* **1962**, *37*, 3489.
(38) Ammeter, J. H.; Bürgi, H.-B.; Thibeault, J. C.; Hoffmann R. *J. Am. Chem. Soc.* **1978**, *100*, 3686.
(39) (a) Mealli, C.; Proserpio, D. M. *J. Chem. Educ.* **1990**, *67*, 399. (b) Mealli, C.; Ienco, A.; Proserpio, D. M. *Book of Abstracts of the XXXIII ICCC*, Florence, 1998; Litografia I.P.: Firenze, 1998; p 510.

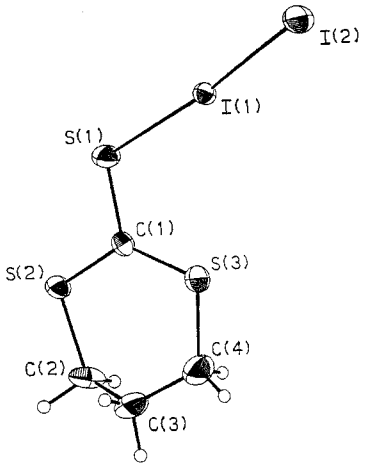

Figure 1. Molecular structure and atom-labeling scheme of the molecule of ptc·I_2. Thermal ellipsoids are drawn at the 30% probability level.

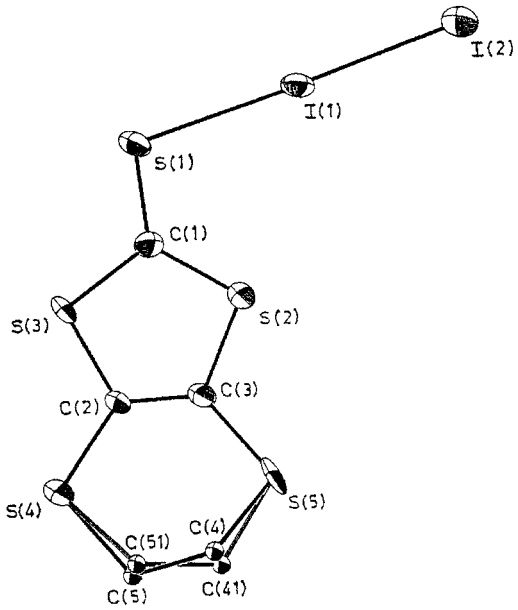

Figure 2. Molecular structure and atom-labeling scheme of the molecule of ttb·I_2. Thermal ellipsoids are drawn at the 30% probability level.

Importantly, I_2 lies almost in the main plane of the ptc molecule. In fact, the SC(S)S and C−S−I−I fragments form a dihedral angle as small as 5.0(2)°.

The shortest contact between iodine atoms of different molecules, 3.986(2) Å (symmetry relation: $1 - x$, $^1/_2 + y$, $^1/_2 - z$), is consistent with chains running parallel to [0 1 0] and held together through the contacts I(1)···S(2) ($-x$, $-y$, $-z$) 3.964(3) Å, I(2)···S(1) ($1 - x$, $-y$, $-z$) 3.890(3) Å, I(2)···S(2) ($1 + x$, $^1/_2 - y$, $^1/_2 + z$) 3.900(2) Å, and C(2)···C(2) ($-x - 1$, $1 - y$, $-z$) 3.52(1) Å. So both the iodine atoms result coordinated in a tetrahedrally distorted way. Only the S(3) atom is not involved in contacts.

ttb·I_2. A view of ttb·I_2 with the atomic labeling scheme is shown in Figure 2. The features of the organic ligand are similar to those observed in its complex with Ag(I).[12] Also in this case the ligand is able to coordinate more than one metal with the both endocyclic and exocyclic sulfur atoms in terminal and bridging modes, and eventually different types of polymers are formed. Although also in this case the exocyclic sulfur atom forms the adduct with iodine, the C═S distance [1.663(8) Å] is only slightly elongated with respect to the same distance in the free ligand [1.633(8) Å[40]]. The five-membered ring is nearly planar [maximum deviation: −0.037(9) Å for C(1)], and so are the sulfur atoms belonging to the six-membered ring [maximum deviation: − 0.059(4) Å for S(5)]. Thus only the C(4) and C(5) atoms forming an ethylenic moiety (disordered) deviate significantly from the main molecular plane [deviations for the two images C(4)−C(5) and C(41)−C(51): 0.82(2) and 0.15(3) Å, 0.07(3) and 0.70(3) Å, respectively]. In view of the latter parameters, the six-membered ring adopts two alternative half-boat conformations, and a different geometry at the S(4) and S(5) atoms is observed.

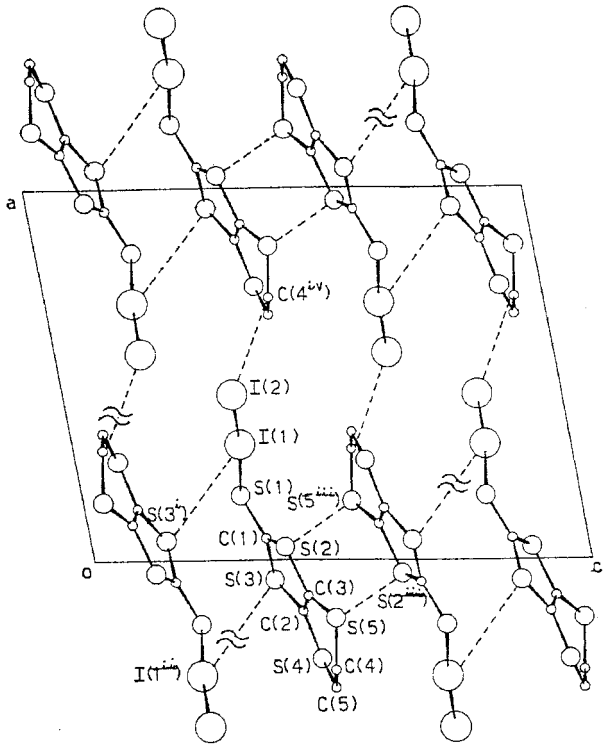

Figure 3. Projection of the structure of ttb·I_2 along [0 1 0].

The S−I−I fragment is roughly linear [175.43(6)°], but, opposite to what is found for the ptc·I_2 structure, the I_2 molecule is almost perpendicular to the SC(S)S moiety (the torsion angle at the S−I vector is now 112.9(7)°). Conversely, the different orientation of I−I does not affect significantly the geometric parameters important for discussion, namely, the lengths of the S−I and the I−I vectors, which are now 2.805(3) and 2.812(2) Å, respectively. While the former is slightly longer, the I−I distance is equal in the two cases. Essentially, the general correlation between d(C−S) and d(S−I) drawn from the comparison of many structures[3b] holds in the present cases as well.

The packing, Figure 3, is determined by the contacts I(1)···S(3^i) ($-x$, $^1/_2 + y$, $^1/_2 - z$) 3.888(3) Å, I(2)···S(1) (x, $1 + y$, z) 3.747(3) Å, S(2)···S(5^{iii}) ($-x$, $1 - y$, $1 - z$) 3.517(5) Å, and S(4)···S(5) (x, $y - 1$, z) 3.532(5) Å forming layers parallel to (1 0 0), which are held together through the contact I(2)···C(4^{iv}) ($1 + x$, y, z) 3.70(2) Å. The coordination around the iodine atoms results as T-shaped. This arrangement is a consequence of the interaction of the central iodine atom I(1) with S(3^i) and is derived from a trigonal-bipyramidal geometry. This geometry is expected for a hypervalent iodine atom (10-

(40) Drew, M. G. B.; Kisenyi, J. M.; Parish, R. V. *J. Chem. Soc., Dalton Trans.* **1987**, 1605.

Table 4. Selected IR (KBr Pellets) and Raman Peaks (cm^{-1}) of ttb, ptc, and Their Diiodine Adducts with I_2 and IBr Tentative Assignments (Approximate Description of the Vibrations)

	ν(C═C)		ν(C═S)		$\nu_s(CS_3)$	
	IR	Raman	IR	Raman	IR	Raman
ptc			993s, 934s	1003m	507w	505m
ptc·I_2			988m, 978s, 945vs	947mw	507w	506s
ptc·IBr			983m, 938vs	n.o.	510w	510ms
ttb	1477m	1479vs	1062vs, 1042s, 1015m, 996w	1052w, 1036m, 1016w	524 m	524s
ttb·I_2	n.o.[a]	1461vs	1065m, 1029vs	1016m	534mw	532vs
ttb·IBr	n.o.	1461ms	1056w, 1015w, 1005w, 988m, 978s, 945vs	n.o.	n.o.	538m

[a] Not observed.

I-3),[41] when I(1) is considered the central atom and the two lone pairs occupy equatorial positions. In the free ligand[42] similar short intermolecular S···S contacts are responsible for the formation of stacks, while the transverse intermolecular contacts are achieved through the interaction of one thionic sulfur with one endocyclic sulfur of the six-membered ring. BEDT-TTF[43] and its conducting salts[44] show a characteristic two-dimensional array of BEDT-TTF, where stacks are similarly formed but the sulfur atoms are also responsible for transverse intermolecular contacts.

Vibrational Spectroscopy. Below 200 cm^{-1}, the $CHCl_3$ solution Raman spectra of ptc and ttb with I_2 show the presence of a single peak at 164 and 162 cm^{-1}, respectively. As mentioned, the observed shift of the frequency of uncoordinated diiodine (ν = 209 cm^{-1} in $CHCl_3$) upon coordination is in accordance with a charge-transfer adduct of type **1**.[45,46] In the same region, the FT-Raman spectra of both ptc·I_2 and ttb·I_2 show a strong peak in the solid state at 146 cm^{-1} (the corresponding adducts with IBr show the ν(IBr) at 151 and 155 cm^{-1}), thus suggesting that the donor−acceptor interaction in the two adducts is almost the same. Moreover, it is stronger in the solid state than in solution.

Raman spectra of diiodine adducts of imidazole-2-thione derivatives in $CHCl_3$ solution[3] show peaks at longer wavenumbers near 150 cm^{-1}, suggesting that their interaction with diiodine is stronger than that in cyclic trithiocarbonates. This is in accordance with the lower electron-donating properties of the sulfur with respect to the nitrogen atoms adjacent to the thione group.

The other IR and Raman bands that are most significant in investigating the donor−acceptor interaction are related to the CS vibrations. Taking into account previous assignments by Klaboe et al.,[47] Dyer et al.,[48a] and Kozlov et al.,[48b] a tentative assignment of these vibrations is given in Table 4. However, it must be pointed out that the assignment to any one mode of vibration of the C═S group is not unequivocal and the description of the bands can be only approximate, since the C═S stretch couples significantly with other modes. This has been emphasized previously by Dyer et al.[48a] in the discussion of the FT-Raman spectra of 1,3-dithiole-2-thione and related species. A recent assignment by Munakata et al.,[12] based on previous reports,[40] of the band found in ttb at 1477 cm^{-1} to ν(C═S) is clearly unreliable. This band, which can be assigned to ν(C═C), is absent in ptc and is found in the Raman spectrum of BEDT-TTF at 1498 cm^{-1}.

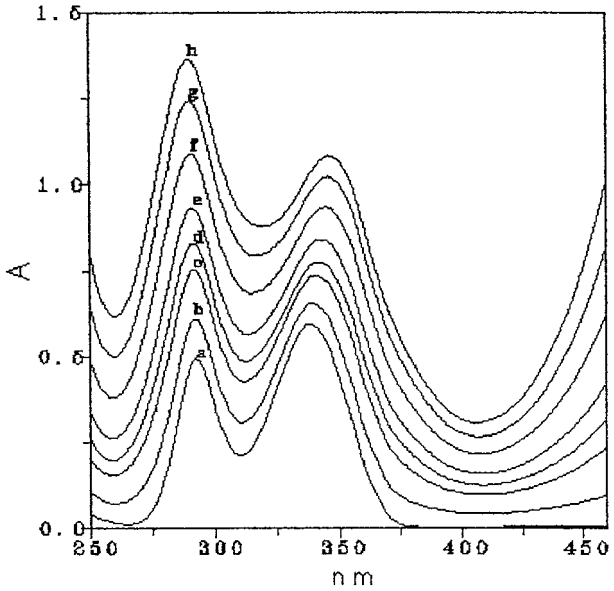

Figure 4. UV−visible spectra at 293 K in 0.1 cm silica cell of $CHCl_3$ solutions containing fixed amounts of ptc ($c = 5.0 \times 10^{-4}$ mol cm^{-3}) and variable I_2 concentrations in the ratios (a) 1:0, (b) 1:4, (c) 1:10, (d) 1:15, (e) 1:20, (f) 1:30, (g) 1:40, (h) 1:50 in the range 250−460 nm.

Solution Studies. The UV−visible spectra of two sets of solutions with a fixed donor concentration (ptc and ttb) and varying concentrations of diiodine in $CHCl_3$ solutions were measured at six different temperatures in the 10−35 °C range. A typical example of the spectra of ptc + I_2 and ttb + I_2 systems are shown in Figures 4 and 5, respectively. A calculation with the program SUPERSPEC[4] (an evolution of the program SUPERQUAD[15]) provided at one time the molar absorptivity of any given species (ϵ_i) and the equilibrium constants (β). This program, similarly to others, is based on the validity of the equation $A = l\sum c_i\epsilon_i = l\sum f_i(\beta)\epsilon_i$ which is derived from the well-known Lambert−Beer law (A is the absorbance at a given wavelength, l is the optical path length, and c_i and ϵ_i are the molar concentrations (function of β) and the molar absorptivities, respectively). The equation is nonlinear with respect to the parameters β and ϵ_i to be determined. Moreover, since the latter are expressed as a product, a strong correlation is expected and the least-squares minimization process may fail if the matrix of the normal equations becomes nearly singular. Such a

(41) 10-I-3 means that the central iodine atom has 10 valence electrons and coordinates three groups. Perkins, C. W.; Martin, J. C.; Arduengo, A. J., III; Lau, W.; Alegria, A.; Kochi, J. *J. Am. Chem. Soc*. **1980**, *102*, 7753.
(42) Larsen, S.; Thorsteinsson, T.; Bowadt, S.; Hansen, T. K.; Varma, K. S.; Becher, J.; Underhill, A. *Acta Chem. Scand.* **1991**, *45*, 709.
(43) Kobayashi, H.; Kobayashi A.; Sasaki, Y.; Saito, G.; Inokuchi H. *Bull. Chem. Soc. Jpn.* **1986**, *59*, 302.
(44) Williams, J. M.; Wang, H. H.; Emge, T. J.; Geiser, U.; Beno, M. A.; Leung, P. C. W.; Carlson, K. D.; Thorn, R. J.; Schultz, A. J.; Whangbo, M.-M. *Prog. Inorg. Chem.* **1987**, *35*, 51.
(45) Klaboe, P. *J. Am. Chem. Soc.* **1967**, *89*, 3667.
(46) Deplano, P.; Devillanova, F. A.; Ferraro, J. A.; Isaia, F.; Lippolis, V.; Mercuri, M. L. *Appl. Spectrosc.* **1992**, *46*, 1625.
(47) Borch, G.; Hendriksen, L.; Nielsen, P. H.; Klaboe, P. *Spectrochim. Acta* **1973**, *29A*, 1109.
(48) (a) Dyer, C. D.; Kilburn, J. D.; Maddams, W. F.; Walker, P. A. *Spectrochim. Acta* **1991**, *47A*, 1225. (b) Kozlov, M. E.; Porkhodnia, K. I.; Yurchenko, A. A. *Spectrochim. Acta* **1987**, *43A*, 323.

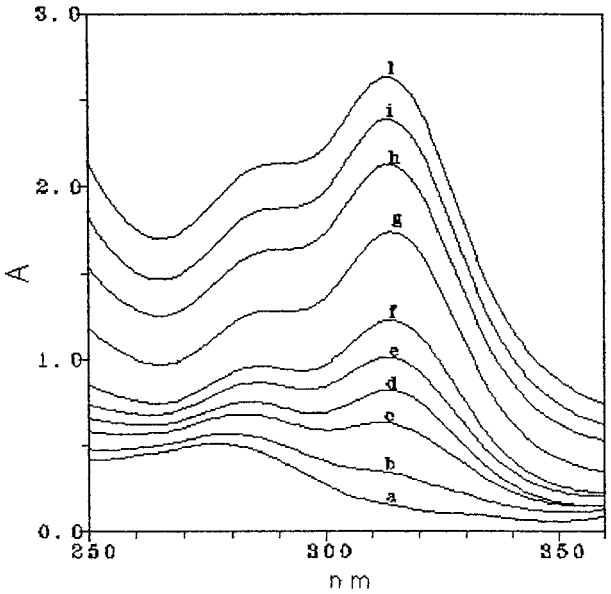

Figure 5. UV−visible spectra at 293 K in 0.1 cm silica cell of $CHCl_3$ solutions containing fixed amounts of ttb ($c = 7.5 \times 10^{-4}$ mol cm^{-3}) and variable I_2 concentrations in the ratios (a) 1:0, (b) 1:1, (c) 1:3, (d) 1:5, (e) 1:7, (f) 1:10, (g) 1:20, (h) 1:30, (i) 1:40, (l) 1:50 in the range 250−360 nm.

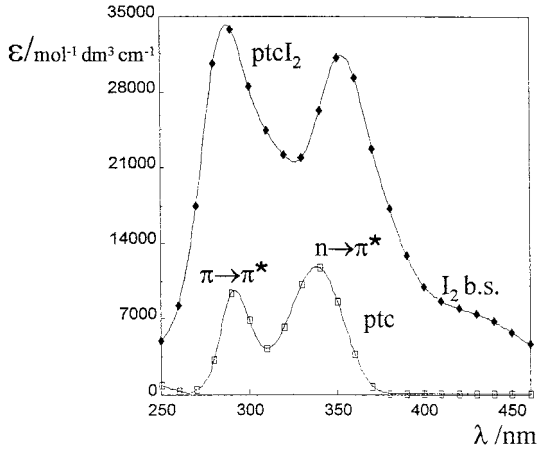

Figure 6. Calculated UV−visible spectrum of the 1:1 complex (ptc·I_2) between ptc and I_2 at 293 K in $CHCl_3$ solutions. The spectrum of the free ligand (ptc) is reported for comparison. The assignments are shown over the bands. I_2 b.s. means blue-shifted I_2 band.

correlation problem may be resolved by recording the spectra of different solutions with a wide range of mutual molar ratios between the absorbing species. Unfortunately measurements using a fixed diiodine concentration and varying concentrations of the donors could be performed only for the ttb case and in a rather narrow molar ratio range, due to the significant absorptivity of the donors in the explored wavelength range. Moreover, as shown in Figures 4 and 5, the bands of the adducts merge with those of the free donors, thus introducing another source of correlation in the calculations. Anyway, convergence is attained for all temperatures by analyzing the data with SUPERSPEC and by assuming that a 1:1 complex (donor·I_2) is present at equilibrium. The refined spectra of the 1:1 complexes of I_2 with ptc and ttb are reported in Figures 6 and 7. The assignment of the bands in the free ligands and in the adducts, also reported in Figures 6 and 7, has been made according to the results of the ab initio calculations. It is noteworthy that the charge-transfer band is not recognizable in the ptc·I_2 case. The values of the formation constants of the

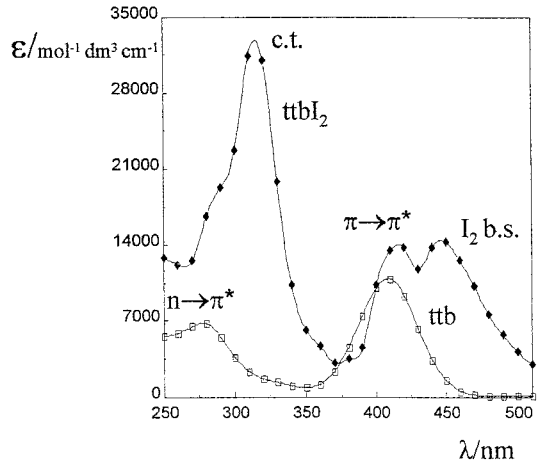

Figure 7. Calculated UV−visible spectrum of the 1:1 complex (ttb·I_2) between ttb and I_2 at 293 K in $CHCl_3$ solutions. The spectrum of the free ligand ttb is reported for comparison. The assignments are shown over the bands. I_2 b.s. means blue-shifted I_2 band.

Table 5. Logarithms of the Equilibrium Constants (Standard Deviations in Parentheses) Calculated by Means of SUPERSPEC and Standard Enthalpy and Entropy Changes for the 1:1 Complexes between ttb and ptc with I_2 in $CHCl_3$ Solutions

	log β	
T /°C	ptc·I_2	ttb·I_2
10	1.81(1)	2.29(1)
15	1.71(1)	2.13(1)
20	1.62(1)	2.04(1)
25	1.52(1)	1.94(1)
30	1.40(1)	1.83(2)
35	1.26(2)	1.67(1)
$\Delta H°$/(kJ mol^{-1})	−42(2)	−45(2)
$\Delta S°$/(J K^{-1} mol^{-1})	−105(8)	−109(4)

[a] Values obtained via van't Hoff equation.

complexes and those of the enthalpy and entropy changes interpolated from the van't Hoff plot (correlation coefficients > 0.99) are listed in Table 5. However, due to the experimental constraints described above we take these as very approximate values. (Using a narrower range of mutual molar ratios, significantly different thermodynamic parameters of the formation equilibria of the two adducts have been found.) The obtained values of $\Delta H°$ are comparable with those reported for imidazole-2-thiones−diiodine[3,4,49] equilibria, while the formation constants are much lower. Differences in $\Delta S°$ and in solvation contributions could be invoked to explain this behavior. However, besides the problems cited above, $\Delta H°$ values of reactions in low-boiling solvents are too approximate to attempt meaningful comparisons due to the narrow temperature range used in their evaluation. Raman spectroscopy (see discussion above) seems more diagnostic in comparing the relative strength of the adducts.

MO Calculations and Their Interpretational Aspects. All of the computational details are reported in the Experimental Section.

Ab initio calculations have been performed at various levels of theory to reproduce the geometries of two adducts between diiodine and the two ligand molecules ptc and ttb which both contain the trithiocarbonate group incorporated in a cycle. The HF (Hartree−Fock) and DFT (density functional) methods have been adopted. One set of HF calculations has been also carried out by using the effective core potential for the heavier atoms.

(49) Suszka, A. *J. Chem. Soc., Perkin Trans. 2* **1985**, 531.

Table 6. Experimental and Calculated Structures

	exptl	B3LYP/ 3-21G**	HF/ 3-21G(*)	ECP/ LANL2DZ
(a) Compound $C_4H_6I_2S_3$ (ptc·I_2)				
Bond Distances/Å				
I(1)−I(2)	2.812(1)	2.794	2.710	2.852
I(1)−S(1)	2.755(2)	3.050	3.560	3.358
S(1)−C(1)	1.690(6)	1.674	1.642	1.667
S(2)−C(1)	1.698(6)	1.749	1.740	1.792
S(2)−C(2)	1.805(6)	1.848	1.821	1.885
S(3)−C(1)	1.690(6)	1.740	1.738	1.791
S(3)−C(4)	1.806(7)	1.849	1.821	1.886
C(2)−C(3)	1.493(10)	1.538	1.532	1.535
C(3)−C(4)	1.433(10)	1.537	1.532	1.535
Angles/deg				
S(1)−I(1)−I(2)	175.42(4)	178.3	176.1	177.1
C(1)−S(1)−I(1)	110.8(2)	107.0	113.9	116.7
C(1)−S(2)−C(2)	107.5(3)	107.7	107.6	109.3
C(1)−S(3)−C(4)	106.0(3)	107.5	107.7	109.5
S(3)−C(1)−S(1)	119.2(3)	118.4	117.5	119.1
S(3)−C(1)−S(2)	128.1(3)	126.4	125.9	122.8
S(1)−C(1)−S(2)	112.7(3)	115.1	116.5	118.1
C(3)−C(2)−S(2)	114.3(5)	114.3	114.8	114.2
C(4)−C(3)−C(2)	115.6(7)	110.8	110.4	112.3
C(3)−C(4)−S(3)	117.6(6)	114.8	114.8	114.1
(b) Compound $C_5H_4I_2S_5$ (ttb·I_2)				
Bond Distances/Å				
I(1)−I(2)	2.812(2)	2.796	2.709	2.841
I(1)−S(1)	2.805(3)	3.023	3.554	3.458
S(1)−C(1)	1.663(8)	1.666	1.638	1.656
S(2)−C(1)	1.699(9)	1.747	1.731	1.788
S(2)−C(3)	1.748(8)	1.769	1.760	1.814
S(3)−C(1)	1.714(8)	1.747	1.732	1.788
S(3)−C(2)	1.742(8)	1.766	1.760	1.814
S(4)−C(2)	1.744(8)	1.769	1.762	1.807
S(5)−C(3)	1.736(9)	1.768	1.762	1.807
S(5)−C(4)	1.76(2)	1.835	1.813	1.877
S(4)−C(5)	1.79(2)	1.837	1.813	1.878
C(2)−C(3)	1.34(1)	1.356	1.328	1.312
C(4)−C(5)	1.57(3)	1.545	1.539	1.534
Angles/deg				
S(1)−I(1)−I(2)	175.43(6)	176.0	179.8	179.1
C(1)−S(1)−I(1)	102.8(3)	100.6	109.5	115.8
C(1)−S(2)−C(3)	97.5(4)	96.7	96.8	96.9
C(1)−S(3)−C(2)	97.8(4)	97.2	96.9	96.8
C(2)−S(4)−C(5)	99.7(8)	100.2	100.4	102.4
C(3)−S(5)−C(4)	98.1(7)	100.2	100.4	102.3
S(1)−C(1)−S(2)	126.3(5)	125.1	123.9	124.5
S(2)−C(1)−S(3)	113.2(5)	113.5	113.5	112.1
S(3)−C(2)−C(3)	115.2(6)	115.9	116.4	117.1
S(4)−C(2)−C(3)	127.9(7)	129.1	128.9	128.5
S(5)−C(3)−C(2)	127.3(6)	128.9	128.9	128.6
S(5)−C(4)−C(5)	114.8(16)	112.3	112.4	112.4
S(4)−C(5)−C(4)	114.4(15)	112.3	112.4	112.4

Also for comparative purposes, the free ptc and ttb molecules have each been optimized separately.

Table 6 summarizes experimental and computed geometries for both adducts ptc·I_2 and ttb·I_2. It is evident that in any case the HF method does not provide a satisfactory agreement and that the best models are obtained from the density functional B3LYP/3-21G** approach. In particular, the S−I distance which can be considered a sensor for the strength of the adduct is difficult to reproduce. The HF calculations provide abnormally long separations (almost to the limit of dissociation). Although more satisfactory, the distances optimized at the DFT level exceed still the experimental ones by 0.22 and 0.30 Å in the ttb·I_2 and ptc·I_2 structures, respectively. Similar discrepancies between calculated (ab initio) and experimental N−I distances of adducts of I_2 with nitrogen bases have been pointed out recently.[50] A possible explanation is that the available basis sets for a highly polarizable element such as iodine are not totally adequate as yet.

Another structural detail to be pointed out is that in all calculations the optimized geometry shows the I_2 molecule to be coplanar with the CS_3 unit independently from the starting point. Conversely, the X-ray structure of the adduct ttb·I_2 shows the upright conformation as the preferred one.

The binding energies between the I_2 molecule and the ptc or ttb ligands are comparable for each set of ab initio calculations. In Table 7, the total energies of the optimized ptc and ttb ligands, of the I_2 molecule and of their adducts are reported. Also the binding energies, for each different computation, are presented as differences between the total energy of the adduct and the sum of the total energies of the donor and the acceptor. The comparison of these data with the standard enthalpy of formation (see Table 5) shows that again the DFT functional provides the best prediction whereas the HF approach strongly underestimates the binding energies (near the dissociation limit).

In order to describe in a chemically intuitive manner the mutual influence of the atoms in the linear S−I−I arrangement, we have performed a parallel qualitative MO analysis by extracting perturbation theory arguments from EHMO calculations. Importantly, the agreement of the latter with the ab initio calculations is good especially in reproducing the composition of the frontier MOs. The attention is focused on the σ MOs which seem to govern the correlated S−I and I−I linkages. Several points have been raised already by Hoffmann et al.,[8] who have recently addressed the electronic nature of I_3^- and the electronegativity effects in the X−I−I$^-$ analogues (X = halogen). Still our analysis will underline the role of both the s and p orbitals at the central iodine atom in fixing the relations between the two σ bonds departing from it. In particular, the effects on varying the donor's capability are pointed out.

Scheme 1 reproduces the interaction among three FMOs which involves mainly the lone pair of the donor (left side) Φ_D and both the filled and empty σ and σ^* combinations of I_2. The latter are made prevailingly of the iodine p axial orbitals with some s orbital contribution. Notice, in particular, that the I_2 σ and σ^* levels are hybridized outward and inward, respectively. In particular, the former has lone pair character besides that of a bonding MO. This is consistent with the fact that two lower and filled σ MOs (cylindrically symmetric and largely based on s atomic orbitals) concur already to define the I−I bond and the second out-pointing σ lone pair of I_2. The latter MO does not appear in Scheme 1.

The perturbation of the donor (left side) induces substantial mixing between σ and σ^* with major consequences for the nature of the central MO σ_2 in the adduct. As shown in the box for σ_2, the central s orbital sums up from both the I_2 components while the p orbital contribution is cut off although it vanishes only in the case of I_3^- (as imposed by symmetry). The overall antibonding character of σ_2, implicit in the phase of the central s orbital (its weight is at least 10%, as found out from the ab initio calculations, see below), becomes directional as the central p orbital mixes in. The phase of the latter depends on the prevailing contribution of the σ or σ^* level as evidentiated in the box of Scheme 1. Also, the relatively high energy of σ_2 (usually the HOMO) is lowered on elongating both the D−I_{centr} and I_{centr}−I_{term} distances or one of them, preferentially. In fact, the closer is the energy of Φ_D to $\sigma^*(I_2)$, the more electron density is driven into the latter and the more the I−I bond elongates (Chart 1a). For example, an X-ray structure of the

(50) Tachikawa, H.; Komatsu, E. *Inorg. Chem.* **1995**, *34*, 6546.

Table 7. Total Energies (au) and Binding Energies (kJ/mol) of the Adducts

computation	I_2	ligand	ligand − I_2	Δ
		(a) Compound $C_4H_6I_2S_3$ (ptc·I_2)		
HF/ECP	−22.311 851	−184.518 210	−206.833 626	−9.37
HF/3-21G(*)	−13 775.836 046	−1 341.089 249	−15 116.930 580	−13.89
B3LYP/3-21G**	−13 771.286 073	−1 344.218 752	−15 125.518 310	−35.40
		(b) Compound $C_5H_4I_2S_5$ (ttb·I_2)		
HF/ECP	−22.311 851	−240.928 399	−263.242 822	−6.74
HF/3-21G(*)	−13 775.836 046	−2 168.905 869	−15 944.746 678	−12.51
B3LYP/3-21G**	−13 781.286 073	−2 173.567 115	−15 954.866 940	−36.11

Scheme 1

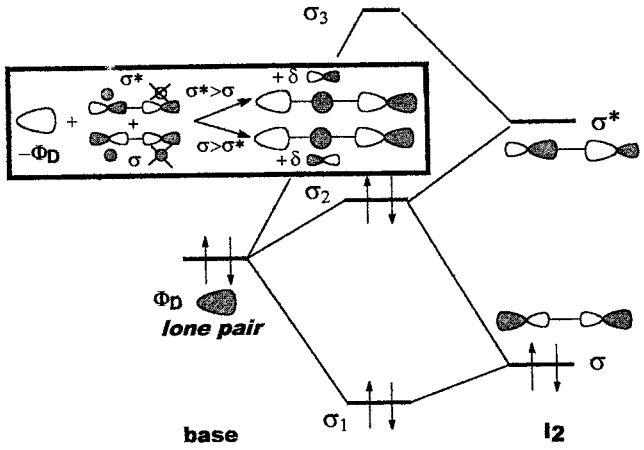

Chart 1

adduct $Me_2PhP{\cdot}I_2$[51] shows that the phosphine (its lone pair is diffuse and relatively high in energy) stretches the I−I distance up to the dissociation [ca. 3.408(2) Å] while the P−I distance is as short as 2.410(2) Å. Peculiarly, the dihalogen or interhalogen adducts of trisubstitued phosphines have been proposed as adducts between the halophosphonium acceptor and the lateral halide donor.[52] By contrast a poorer amine donor barely stretches the I−I linkage. For instance, in the structure of Me_3NI_2[53] the I−I distance is only 2.83 Å while the N−I bond length is 2.27 Å. Although apparently short, the latter is definitely more stretched than the corresponding P−I distance in view of the 0.3 Å difference between N and P covalent radii. Remarkably all of the structures where the I−I linkage is stretched almost to the point of ion pair dissociation (e.g., R_3PI^+ and I^-) are characterized by a short contact between the quasi-free iodide anion and a third group with residual positive charge (this is often the P atom of a second phosphonium group).[51]

As mentioned, a symmetry-imposed balance of the σ/σ^* contributions in σ_2 (with disapparence of the central p orbital) occurs in the case of I_3^-, hence the origin of the classical three-orbital/four-electron model. If, on one side, a less electronegative and stronger donor than an iodine atom itself can trigger I−I elongation and eventually its cleavage, a weaker donor interacts preferentially with the I_2 σ level. The outward hybridization of the latter component persists in σ_2 so that the $D-I_{central}$ antibonding relationship is rather effective (see Chart 1b). In this case, the barrier due to the repulsion between the donor and the I_2 out-pointing lone pairs is not yet canceled out.

Scheme 2

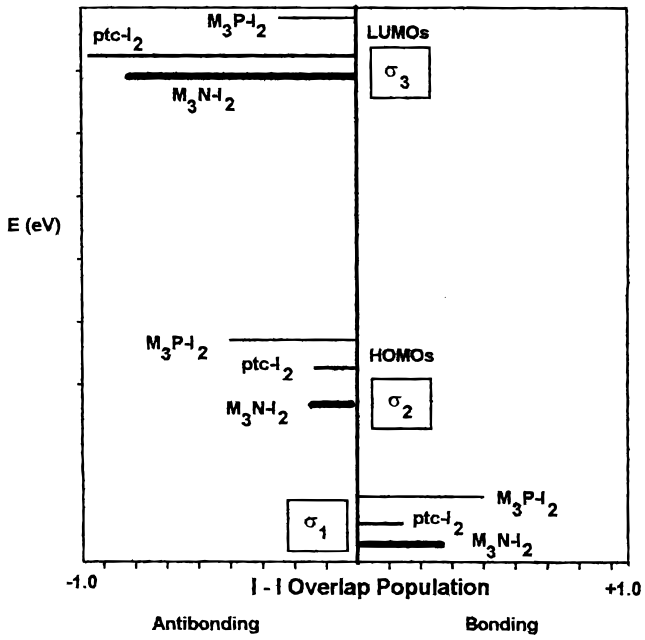

For their simplicity as models and for the amount of available structural data, the adducts $R_3N{\cdot}I_2$ and $R_3P{\cdot}I_2$ define two limiting situations (a detailed quantitative and qualitative MO analysis of these models will be reported elsewhere[54]). Scheme 2 is extracted from three calculated and superimposed MOOP diagrams (for the amine, phosphine, and ptc adducts, respectively) which can be easily produced with the new version of the program CACAO.[39] In these diagrams, the contribution of the single MOs to the I−I overlap population (the separation between the two iodine atoms is in all cases fixed at 2.8 Å) is graphically shown. In particular, Scheme 2 presents only the contribution given by the σ_1, σ_2, and σ_3 MOs in Scheme 1 (incidentally, the amount of bonding contribution to I−I shown by σ_1 already involves the contribution of other MOs which lie even deeper in energy).

Scheme 2 reads as follows. The phosphine donor confers the strongest antibonding character to the HOMO in line with the hybridization of the central iodine atom (see Chart 1a). Interestingly, the I−I σ^* character appears small in the LUMO of $R_3P{\cdot}I_2$ (σ_3) thus indicating that the I−I bonding is almost null (at the limit of cleavage). For the adduct with an amine, the direction of the central hybrid is inverted (Chart 1b) so that the HOMO has prevailing N−I antibonding character. In this case, the I−I σ^* character is transferred into the empty σ_3 level, which eventually accounts for the greater amount of I−I bonding.

(51) Bricklebank, N.; Godfrey, S. M.; Lane, H. P.; McAuliffe, C. A.; Pritchard, R. G.; Moreno, J. M. *J. Chem. Soc., Dalton Trans*. **1995**, 2421.
(52) Deplano, P.; Godfrey, S. M.; Isaia, F.; McAuliffe, C. A.; Mercuri, M. L.; Trogu, E. F. *Chem. Ber*. **1997**, *130*, 299.
(53) Stromme, K. O. *Acta Chem. Scand*. **1959**, *13*, 268
(54) Deplano, P.; Ienco, A.; Mealli, C.; Pintus, G. Work in progress.

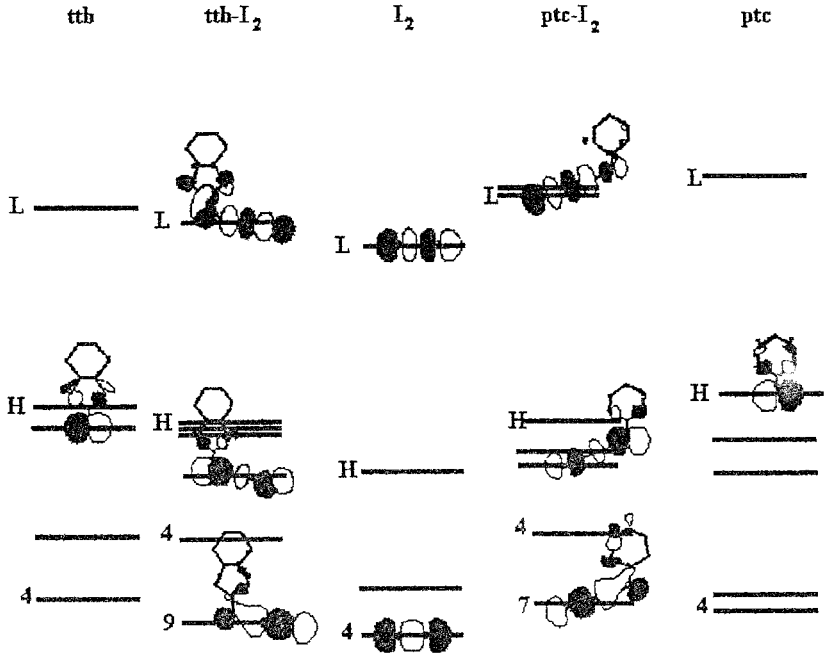

Figure 8. Diagram of the energy levels of ttb, ptc, I_2, and their adducts. The number reported on the side of the level indicates the position of that orbital under the highest occupied molecular orbital, while the letters H and L refer to the HOMO ahd LUMO, respectively; the numbering of the orbitals without labels is obtained by counting the number of orbitals intervening between the HOMO and the actual orbital.

It is clear from Scheme 2 that the strength of the exocyclic sulfur atom of the CS_3 group in the ligands ptc and ttb is more comparable to the amine than to the phosphine ligand, the qualitative MO results being quite consistent with the experimental X-ray data.

A reliable confirmation of the above picture can be obtained by the DFT calculations. Figure 8 summarizes several aspects of the latter by reporting the diagrams of the energy levels of the separated molecules ttb, ptc, and I_2 as well as of the adducts (the number at some specific level is indicative of the relative order below the corresponding HOMO). In addition, several drawings illustrate the nature of some of the relevant MOs. By first focusing on two of the highest occupied MOs of the two adducts with I_2 (HOMO−3 for ttb·I_2 and HOMO−2 for ptc·I_2), it becomes evident that the contribution of the s orbital of the central iodine atom (∼10% in both MOs) is such to cause more S−I than I−I antibonding.

Perhaps the most important point to be made from the above considerations is that the extended linkage over the linear system D−I−I cannot be limited to the widely accepted three-orbital/four-electron model. Rather the role of all of the eight σ electrons (the two bonding ones plus two lone pairs at I_2 as well as the lone pair of the donor) must be considered. Since one electron pair at the terminal iodine atom points outward, only the remaining six electrons are shared by four σ components (namely two in-pointing σ hybrids at the lateral I and D atoms plus the s and p atomic orbitals of the central iodine atom). In summary, the extended D−I−I interaction can be conveniently described as a four-orbital/six-electron model whose delocalization rules we have tentatively described above.

Back to Figure 8, besides the MOs drawn, we wish to add the following comments about the nature of the other levels.

(i) The HOMO and HOMO−1 of the isolated I_2 molecule are as expected the degenerate pairs of antibonding π^* and bonding π orbitals.

(ii) In ttb the HOMO−4 is a π orbital extending over the atoms S(2)C(3)S(5) and S(3)C(2)S(4); the HOMO−2 is the π bonding orbital for the exocyclic C═S linkage; the HOMO−1 is the in-plane lone pair at the atom S(1). The HOMO and LUMO coincide with the C═C π bonding orbital (the linkage connecting the two rings) and with the CS_3 π^* level, respectively. Accordingly, the transitions $\pi \rightarrow \pi^*$ (HOMO → LUMO) and n → π^* (HOMO−1 → LUMO) (see Figure 7) can be safely assigned.

(iii) The ttb·I_2 HOMO−4 is the sum of the separate I_2 and C═S π MOs while the HOMO−1 and the HOMO are essentially the iodine molecule degenerate pairs while the HOMO−2 is the sum of the C═C π orbital and the p_π sulfur and terminal external iodine atoms. The blue-shifted diiodine band is thus assigned to the transitions HOMO−1 → LUMO, the charge-transfer band to HOMO−3 → LUMO ($\sigma_2 \rightarrow \sigma_3$ of Scheme 1) while n → π^* and $\pi \rightarrow \pi^*$ are HOMO−3 → LUMO+1 and HOMO−2 → LUMO+1, respectively (see Figure 7).

(iv) The ptc HOMO−4 and HOMO−3 are mixtures of the p_x, p_y, and s atomic orbitals of all of the heavy atoms; the HOMO−2 is the out-of-phase sum of the ring sulfur atoms p_z; the HOMO−1 and the LUMO are analogous to the ttb HOMO−2 and LUMO, respectively. In ptc the p_y lone pair is the HOMO (HOMO−1 in ttb). Thus there is a reversed order of the n → π^* and $\pi \rightarrow \pi^*$ transitions, which are in this case HOMO → LUMO and HOMO−1 → LUMO, respectively (see Figure 6).

(v) The ptc·I_2 HOMO−4 is the I_2 π bonding orbital while the HOMO−3 comprises the C═S π bonding orbitals together with minor p_z components from the ring sulfur atoms; the HOMO−1 and HOMO orbitals are the pair of I_2 π^* orbitals; the LUMO orbital in this adduct is the CS_3 π^* orbital. The blue-shifted I_2 band is thus HOMO−1 → LUMO+1, and the charge-transfer band ($\sigma_2 \rightarrow \sigma_3$) is now HOMO−2 → LUMO+1; while n → π^* and $\pi \rightarrow \pi^*$ are now HOMO−2 → LUMO and HOMO−3 → LUMO, respectively. The sequence of the calculated frequencies is in agreement with that observed.

Conclusions

The present study has shown that (i) only the thionic sulfur is involved in the coordination with diiodine and short S−S intermolecular interactions influence the packing in the ttb·I_2 case only; (ii) Raman spectroscopy has a high diagnostic value in evaluating the strength of the interaction between the donor and the iodine molecule; this becomes especially useful when the experimental restraints do not allow one to obtain fully reliable thermodynamic parameters through spectrophotometric methods; (iii) the ab initio DFT method can reproduce the experimental X-ray structures of the adducts at a satisfactory level; moreover, a reasonable assignment of the visible spectra can be made on the basis of these results; (iv) the qualitative MO analysis can help one to focus more closely on the nature of the extended D−I−I bonding.

In conclusion, it is pointed out the widely accepted *three-orbital/four-electron* model is not totally exhaustive. If on one side Schemes 1 and 2 have highlighted the three levels $\sigma_1-\sigma_3$, it has been also pointed out that the mixing of s and p atomic orbitals at the central iodine atoms is of critical importance. In particular, also the redistribution of the electron density into the second sp hybrid (lower than σ_1 and former lone pair at the now central I atom) must be taken into account. In conclusion, a *four-orbital/six electron* model is more adequate and it can be interpreted by exploiting the principles of perturbation theory.

Depending on the strength of the donor, two limiting situations are outlined. A strong donor could ultimately lead to the formation of the ion pair D−I^+ and I^-. Conversely, there remains a significant four-electron repulsion between the lone pairs of a weak donor and of I_2, when the delocalized D−I−I linkage is formed. Further studies in this field are in progress.

Acknowledgment. The Consiglio Nazionale delle Ricerche (Progetto Finalizzato, Materiali Speciali per Tecnologie Avanzate II) is acknowledged for financial support of this research. Thanks are due to the Area della Ricerca di Firenze for computing time and facilities.

Supporting Information Available: Listing of hydrogen coordinates, isotropic displacement parameters, and anisotropic displacement parameters. This material is available free of charge via the Internet at http://pubs.acs.org.

IC9901867